Stage I of recovery in 5 MeV electron-irradiated iron and iron-chromium alloys: the effect of small cascades, migration of di-interstitials and mixed dumbbells

1999 J. Phys.: Condens. Matter 11 8633

(http://iopscience.iop.org/0953-8984/11/44/302)

J. Phys.: Condens. Matter **11** (1999) 8633–8644. Printed in the UK PII: S0953-8984(99)00128-9

Stage I of recovery in 5 MeV electron-irradiated iron and iron–chromium alloys: the effect of small cascades, migration of di-interstitials and mixed dumbbells

A L Nikolaev

Institute of Metal Physics, Ural Branch Russian Academy of Sciences, S Kovalevskaya Street 18, GSP 170, Ekaterinburg 620219, Russia

E-mail: nikolaev@imp.uran.ru

Received 15 December 1999, in final form 6 July 1999

Abstract. Irradiation of iron with 5 MeV electrons is accompanied by the generation of point defects within small cascades, which changes the shape of the stage I resistivity recovery spectrum and stimulates the formation of di-interstitials that manifest their migration near the I_{D1} substage. The specific features of stage I recovery in concentrated Fe–Cr alloys are discussed in terms of mixed dumbbell formation, migration and trapping in configurations that include several chromium atoms. Resistivity values retained in the alloys at the end of stage I are well described by the trapping of Fe–Cr mixed dumbbells in chromium atom pairs.

1. Introduction

Knowledge of the fundamental properties of point defects is important to understand radiation damage mechanisms in structural materials and thus for the development of alloys suitable for cladding in breeder reactors and as first wall materials in fusion reactors. Ferritic stainless steels are known to be more resistant to swelling than FCC steels; however, the properties of point defects in these materials, especially of interstitial atoms (IAs), have been less investigated than those of austenitic steels. The lack of information about IA properties also hinders understanding of the physical mechanisms involved in the void swelling resistance of ferritic steels.

Electrical resistivity recovery (RR) measurements have shown that some technologically important impurities in dilute iron-based alloys, such as Cr and Mn, interact with self-IAs to form mixed dumbbells that are mobile at temperatures below the onset of long-range self-IA migration [1, 2]. Recently these results have been reproduced in Fe–Cr alloys [3]. IA trapping in configurations including several Cr atoms (configuration trapping) has also been reported [1] in concentrated Fe–Cr alloys, similar to the phenomenon observed earlier in FCC Ag–Zn alloys [4]. Since such trapping can modify significantly the properties of IAs [4, 5], it may be one of the physical mechanisms leading to the swelling resistance of Fe–Cr alloys, and it therefore requires detailed investigation. The first step in such a study might be elucidating basic IA behaviour in stage I in concentrated Fe–Cr alloys by examining the available RR data (1 and 3 at.% Cr [1] and 5, 10 and 15 at.% Cr [6]). But some of these data [6] were obtained with poor temperature resolution (15 K), so some important features of the RR structure could have been missed. That is why we have undertaken a more detailed study of the Cr effect on RR

0953-8984/99/448633+12$30.00

in iron over the stage I temperature interval (80–140 K) in a wide range of Cr concentrations (2–16 at.%).

A series of Fe–Cr alloys has been prepared for such investigations. Data concerning some aspects of the IA configuration trapping in an electron-irradiated Fe–16Cr alloy were published earlier [7]. In this paper, we compare the RR data in iron and the Fe–Cr alloys. Specific features of stage I recovery in iron irradiated with 5 MeV electrons, generating primary knock-on atoms with energies exceeding 1000 eV, are discussed. By analysing the RR in the Fe–2Cr alloy and comparing it with the available RR data [1], we put forward a model describing the behaviour of the IAs over the stage I temperature range and then verify the predictions of the model in the other alloys.

2. Experiment

2.1. Samples

The alloys were prepared from powder carbonyl iron (having main impurities, in at. ppm: C $\sim$ 170, N $\sim$ 70, Ni $\sim$ 100 and Cr $\sim$ 2) and flake refined electrolytic chromium (having main impurities, in at. ppm: C $\sim$ 200, N $\sim$ 200, Al $\sim$ 80, Fe $\sim$ 60). The raw powder mixtures were pressurized and melted. The ingots were forged and hot rolled at about 1000–1050 K into 2.5–3 mm thick plates. About 0.5 mm of the plate surface layer thickness was removed from each side, and the plates were then cold-rolled to a thickness of 70–100 μm. The samples were spark cut from the foils and finally heat treated at 1070 K for 4 h in 10^{-4} Pa oilless vacuum. For more details on the preparation of the samples, refer to [7].

Two types of iron sample were used (table 1). The iron sample labelled Fe1 was prepared from the same raw iron, zone melted (RRR† = 160) and cold rolled, and has RRR = 155. The second sample, labelled Fe2, and used to test alloy contamination, was prepared from material initially intended for the preparation of a dilute Fe–0.2Cr alloy. Because of the large content of oxygen in the raw powder iron, which is not dissolved but forms oxides, the chromium was lost to oxidation, and the material had RRR = 140 after melting‡. The Fe2 sample was then prepared identically to the alloys, as indicated above, and the final RRR value was determined to be 95. The reduction in RRR was probably a result of contamination with impurities during forging and hot rolling of the ingots. Since a surface layer (about 0.5 mm thick) was removed prior to fabricating the final foil samples, it was assumed that these should be fast-diffusing impurities, such as carbon and nitrogen. Further consideration of the RR in the Fe2 sample, as discussed below, supports this assumption.

According to [8], RRR = 160, 107 and 90 ($H = 0$) corresponds to interstitial impurity concentrations of about 30, 100 and 300 at. ppm, respectively. Thus, the Fe1 and Fe2 materials contained no more than 30 and $\sim$200 at. ppm of the interstitial impurities, respectively. The last value is the estimate of the level of alloy contamination with interstitial impurities. It can also be expected that the major fraction of nickel impurities, present in the raw powder iron, passed into Fe1 and Fe2, since the small difference in the solubility of Ni in solid and liquid iron [9] prevents it from being removed during zone refining. Taking the nickel and carbon contributions to the residual resistivity as 2.1 and 4.9 $\mu\Omega$ cm/at.% respectively [2, 10], Fe1 was estimated to contain about 10 at. ppm of interstitial impurities, except for $\sim$100 at. ppm Ni.

† Ratio of resistivities at room temperature and at 4.2 K (without magnetic field).

‡ This reduction in RRR is, most probably, due to the remaining traces of chromium, since simple melting of raw iron under quite different conditions never gives RRR values below 150. For Fe, doped mainly with Ni and interstitial impurities C + N (see below), the observed increase in resistivity corresponds to an addition of 10–15 at. ppm Cr. Also see discussion [1] concerning the effect of impurities on the Cr specific resistivity.

Table 1. Specimen characteristics.

Sample (sample position)[a]	Cr concentration, deduced from: Weight (at.%)	X-ray analysis (at.%)	Residual resistivity (at.%)	Shape factors (at.%)	Thickness (μm)	Residual resistivity ($\mu\Omega$ cm)	Radiation-induced resistivity (90 K) ($\mu\Omega$ cm)
Fe1 (1.1)[b]	—	—	—	—	60	0.065	0.146
Fe2 (1.2)[b]	—	—	—	—	60	0.102	0.133
Fe–2Cr (1.4)[b]	2	2.1 ± 0.04	1.64 ± 0.05	1.7 ± 0.05	45	3.05 ± 0.1	0.294
Fe–4Cr (2.4)[b]	4.3	4.2 ± 0.08	3.97 ± 0.11	3.7 ± 0.11	35	6.99 ± 0.2	0.378
Fe–6Cr (2.3)[b]	6.0	6.1 ± 0.12	6.2 ± 0.3	—	55	9.68 ± 0.3	0.59
Fe–9Cr (2.2)[b]	8.7	9.0 ± 0.18	—	—	65	11.96 ± 0.35	0.6
Fe–11Cr (2.1)[b]	10.7	10.8 ± 0.22	—	—	60	12.27 ± 0.35	0.535
Fe–16Cr (1.3)[c]	15.7	16.1 ± 0.32	—	—	55	12.1 ± 0.35	0.35

[a] The first figure corresponds to the row and the second figure indicates the position in the holder.
[b,c] Irradiation runs I and II respectively.

Alloy residual resistivities were determined on separate samples of suitable form. Unlike [7], where a micrometer was used to measure sample dimensions, an instrumental microscope was used, and a slight curvature of the Fe–16Cr alloy sample stick found. This malformation caused an additional inaccuracy in the measurement of the resistivity [7], which has been accounted for.

The chromium content by weight agrees with that obtained by x-ray fluorescence analysis (table 1). In the Fe–2Cr and Fe–4Cr alloys, the shape factors were deduced both from geometry and from the resistances at room temperature and liquid helium (4.2 K) according to [1]:

$$s = [\rho_{295\ K}(\mathrm{Fe}) + \delta\rho]/[R_{295\ K} - R_{4.2\ K}]$$

where $R_{295\ K}$ and $R_{4.2\ K}$ are the alloy resistances at 295 K and 4.2 K, $\rho_{295\ K}(\mathrm{Fe}) = 10\ \mu\Omega$ cm and $\delta\rho$ ($\mu\Omega$ cm) $= 2.5C$ (at.%), and C is the Cr concentration. Comparison of the obtained values was used to estimate the Cr content in the solid solution (table 1). A resistivity calibration curve was plotted based on available residual resistivities in Fe–Cr alloys up to 15 at.% Cr [1, 11], and the Cr concentrations in the solid solution were also deduced from the residual resistivity of the alloys, according to that curve (table 1). A discrepancy of 0.2–0.3 at.% was found between the total and the solid solution Cr concentrations, as seen in the Fe–2Cr and, probably, Fe–4Cr alloys (table 1), which might be explained by chromium oxidation. The latter was confirmed by nuclear reaction analysis, which found about 0.3 at.% oxygen in our alloys. In the most concentrated alloys, the resistivity was insensitive to such small variations in the chromium content.

Because of deviations from Matthiessen's rule (DMR) in iron-based alloys [12], the apparent Frenkel pair (FP) specific resistivity may depend on the concentration of defects, and the measured radiation-induced resistivity is not always a straightforward measure of the defect concentration [1]. Therefore, the measured experimental data must require, in some cases, a correction [1, 13]. In our iron samples, the main impurities have similar conduction electron scattering characteristics (Ni [12], C + N [7]) as FP [1] and the resistivity data do not require much correction [14]. In concentrated Fe–Cr alloys, the necessity of the correction is defined by the ratio of radiation-induced and residual resistivities (γ). As is shown in figure 8 [1] the marked, but not the principal, correction in the RR in concentrated Fe–1Cr and Fe–3Cr alloys (γ is 15% and 7%, respectively) is necessary only in the Fe–1Cr alloy. Among our samples, only in Fe–2Cr is γ more than 7%, and such a correction is important for the extrapolation shown in figure 3, where it has been taken into account.

2.2. Irradiation and annealing

The samples were mounted in a sample holder in two rows of four, one behind the other, and irradiated at a Linac with 5.5 MeV electrons in a flow-through helium cryostat at temperature about 40–50 K. Two irradiation runs were carried out with 6.6×10^{17} cm^{-2} (run I) and 3.9×10^{17} cm^{-2} (run II) fluences respectively (table 1). The initial concentration of FPs in the samples was about 30–60 at. ppm.

After irradiation, the sample holder was transferred in a special unit into a helium Dewar where the samples were further stepwise annealed in the same unit at an average annealing rate of 1 K min^{-1} in 6–10 K steps (i.e. the value of annealing time in minutes was equal to that of temperature step in K). A comparison of the RR curves of the Fe1 samples irradiated and annealed in the cryostat and irradiated and transferred to a helium Dewar (run I) showed that the recovery spectra in both cases were quite similar, except for heating up to 80 K during transfer. The same estimation of the heating in run I was obtained by comparing the RR data of the Fe–4Cr and Fe–9Cr samples with data in different experiments.

The electrical resistivity was measured at 4.2 K ($H = 0$) with an accuracy about 0.1 nΩ cm and the radiation-induced resistivity increments after annealing at 90 K are listed in table 1. For more details, refer to [7].

3. Results and discussion

3.1. Resistivity recovery in iron

In figures 1 and 2, the integral and differentiated (recovery spectra) RR curves, respectively, for the Fe1 and Fe2 samples are shown. The structure of the recovery spectrum observed in the Fe1 sample over the stage I temperature interval (85–142 K) differs from that of the recovery spectrum in the Fe + 100 at. ppm Ni alloy (which can be considered as the analogue of our Fe1) obtained after irradiation with 1.6 MeV electrons [2] (cf figure 2(a)). The following substages are observed in the latter alloy: I_C—at 89 K, attributed to a recombination of close pairs; I_{D1}—at 101 K, also a recombination of close pairs; I_{D2}—at 108 K, a correlated migration of self-IAs and I_E—at 123–144 K, a long-range self-IA migration (poorly resolved) [10]. In our spectrum, the only clearly resolved broad peak is observed at 110 K, which can be attributed to processes similar to the ones taking place in the I_{D2} substage. Two recovery peaks are observed in Fe1 over the stage II temperature interval (142–200 K)—at 150 and 165 K (figure 2(c)). The first (at 150 K) was observed in iron doped with Ni [2, 14], and the second (at 165 K) was observed in iron doped with carbon [10]. Such a stage II structure correlates with the impurity content (section 2.1) in Fe1.

Over the 125–142 K temperature interval, the RR in the Fe2 sample is slightly suppressed compared to Fe1 (figures 1 and 2(a)), and this suppression corresponds to an increase of the same amplitude in the RR at 165 K (figures 1 and 2(c)). This observation can be explained by the trapping of freely migrating self-IAs by interstitial impurity atoms and the formation of complexes, reducing the RR, with a subsequent dissociation of such complexes at 165 K, accompanied by a recovery in the RR in agreement with [10]. Therefore, over the 125–142 K temperature interval, the free migration of self-IAs is observed in our iron samples during post-irradiation annealing, in agreement with [10].

At the same time, the I_C and I_{D1} substages are not distinctly resolved in our spectra. Moreover, the RR in the Fe2 sample is suppressed at 104 K (figures 1 and 2(a)). This effect is three to four times greater than the scattering in the difference between the RRs in the Fe1 and Fe2 samples (inset in figure 1). As shown in the inset, the reliability of the delay in the RR of

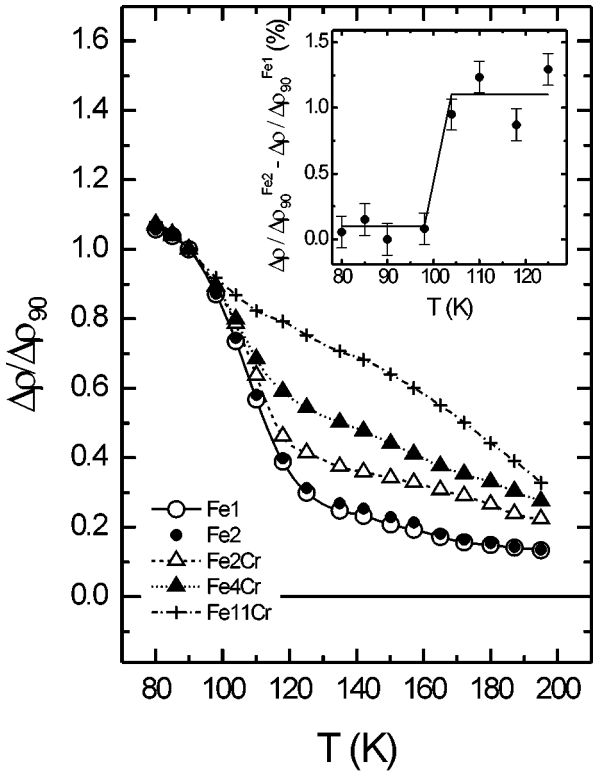

Figure 1. Resistivity recovery curves normalized at 90 K for iron and Fe–Cr alloy samples. In the inset: the difference in resistivity recovery between the Fe1 and Fe2 samples over the substage I_{D1} and I_{D2} temperatures.

the Fe2 sample (as compared to Fe1) is confirmed by three data points below 104 K and by four data points at 104 K and above. The RR suppression at 104 K appears to be defect trapping at the surplus interstitial impurity atoms in Fe2. But such a small impurity atom concentration ($\sim$200 at. ppm) can manifest itself in defect trapping only if a long-range defect migration takes place. Free migration of simple defects at 104 K is not known in iron.

Cr atoms trap IAs and suppress the RR (see the next section). The suppression of the RR rate with Cr doping over range of several per cent is weaker at 104 K than at 110 K (figure 3), which agrees with the close pair and correlated recombination processes that are known to take place near 104 K and 110 K respectively. But the close pair recombination process taking place near 104 K excludes any visible effect on the RR of the impurity atoms in concentration about 200 ppm, in contrast to the observation. Also, the extrapolation of the concentration dependences in figure 3 to a zero chromium content coincides with the data obtained in the Fe1 and Fe2 samples at 110 K and leads to lower values at 104 K. If Cr additions have the same effect as the interstitial impurities on the RR, the experimental data can be explained as the coexistence near 104 K of two processes: the first is a long-range migration of some species, and the second is an ordinary close pair recombination. In concentrated alloys, the long-range migration is totally suppressed, and the extrapolation of the RR rate to a zero chromium concentration should give a lower RR rate value than the one obtained in the experiment.

A comparison of the RR spectra of Fe1 and iron after 1.6 MeV irradiation, shown in figure 2(a), indicates that the close pair recombination substages, I_C and I_{D1}, are slightly

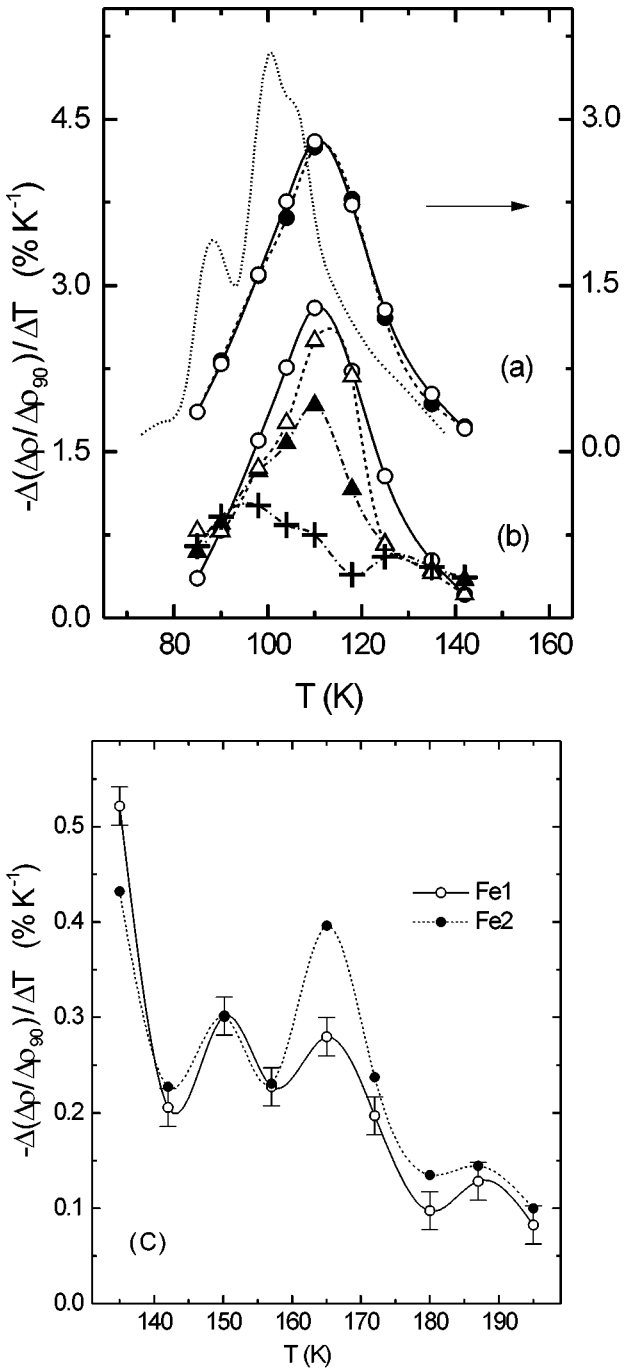

Figure 2. Resistivity recovery spectra over the stage I temperature interval: (a) Fe1 and Fe2 samples (open and black circles) compared with the resistivity recovery spectrum in Fe + 100 at. ppm Ni after 1.6 MeV electron irradiation [2] (dotted curve); (b) in Fe1 and Fe–Cr alloys (from figure 1). (c) Resistivity recovery spectra over the stage II temperature interval in the Fe1 and Fe2 samples.

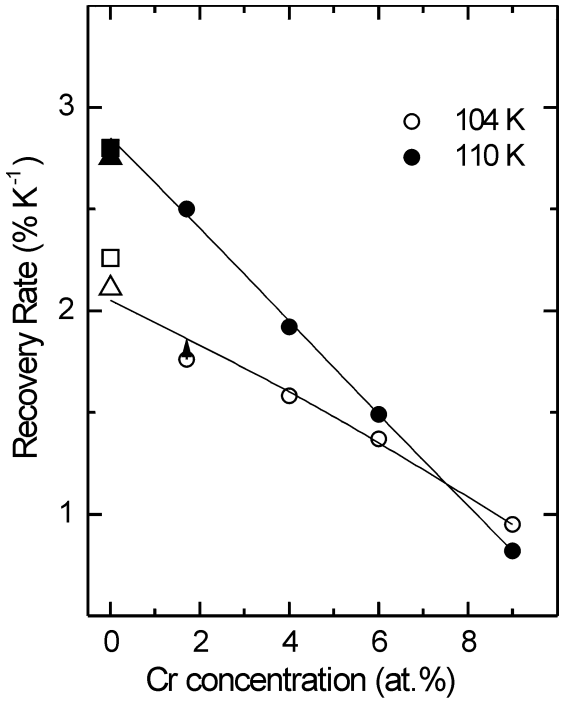

Figure 3. Resistivity recovery rates at 104 K (open symbols) and 110 K (black symbols) in Fe–Cr alloys (circles) against Cr concentration, Fe1 (squares) and Fe2 (triangles). An arrow shows the correction due to DMR in the Fe–2Cr sample.

expressed in the RR of the 5 MeV electron-irradiated iron. The correlated migration substage, I_{D2}, is expanded to higher temperatures: the distinct transition from correlated to free self-IA migration, clearly seen in the dotted curve, is changed to a smooth, continuous transition. This feature of the I_{D2} substage provides evidence of an expansion of the separation distances between FP partners, and such expansion indicates a generation of point defects, not only as separate FPs, but also within small cascades.

According to [15], primary knock-on atoms having energies 300 and 500 eV can generate cascades in α-Fe consisting of five and eight FPs respectively. As a result of point defect generation within cascades, the total fraction of close pairs is reduced. The formation of di-interstitial atoms (DIAs) directly within cascades during irradiation cannot be excluded. According to the calculations of Johnson [16], the DIA migration energy is 0.18 eV. Therefore, the onset of DIA free migration and DIA trapping at interstitial impurities near the I_{D1} substage may be observed in our iron samples. If the apparent coincidence in DIA migration onset and the I_{D1} substage is fortuitous, then the onset temperature corresponds to the DIA migration energy, about 0.25 eV. However, there are essential reasons to think that this coincidence is not fortuitous.

In Fe [17], as in Mo [18], the easiest mode for dumbbell migration is a (110) planar mode. Therefore the FP partners, located in different easy migration planes at distances larger than the spontaneous recombination radius and smaller than the capture radius, form bound close pairs. For final recombination, the dumbbell requires additional thermal stimulation to rotate and to jump out of its easy migration plane towards a vacancy. Such rotation takes place in the I_{D1} substage. Some self-IAs within the same cascade may also form similar bound close

pairs, i.e. the close neighbouring self-IAs located within each others' capture volume but with a mutual orientation different from the one necessary for DIA formation [16]. In that case, DIA formation needs dumbbell rotation and thus is similar to the close pair recombination in the I_{D1} substage. In such a situation, the DIA actual migration energy might be lower than 0.25 eV, since DIA migration might be retarded by the dumbbell reorientation process, and the coincidence in DIA migration and the I_{D1} substage would be not fortuitous. In fact, if the mutual dumbbell orientation in the IA close pairs is stochastic, then only a minor portion of the IA close pairs will become DIAs immediately after formation, and the majority will transform into DIAs only in the I_{D1} substage, giving rise to the DIA migration. Therefore, if the mutual dumbbell orientation in the IA close pairs is stochastic, the observed coincidence is very strong evidence in favour of the process discussed.

It is likely that the excess resistivity retained in the Fe2 sample after trapping of DIAs at 104 K recovers above 165 K, since at 195 K, the percentage of the RR in both iron samples is identical (figure 1). The enhanced RR at 180–195 K (figures 1 and 2(c)) can probably be attributed to a release of trapped DIAs at interstitial impurities. A detrapping peak was also found in 3 MeV electron irradiated carbon doped iron [10] in the same temperature range. This peak was clearly expressed when the concentration of IAs was significantly below the concentration of carbon atoms. Such a situation might be favourable for the formation of DIA–carbon atom complexes during dissociation of the IA–carbon atom ones near 165 K. Therefore, it cannot be excluded that the 185 K peak is also associated with the release of trapped DIAs, but a more reliable interpretation of the process requires data from special experiments.

3.2. Resistivity recovery in Fe–Cr alloys

Doping with chromium over range of several per cent concentration produces a progressive suppression in the total RR (figure 1) and in the RR rate over the stage I temperature interval (figure 2(b)). This effect is significantly more important than the effect of the impurity contamination, and therefore it can be concluded that the chromium atoms capture IAs and suppress the RR, in agreement with [1].

Figure 2(b) shows that RR suppression in the Fe–2Cr alloy is not the same over the stage I temperature range, since near 118 K, the RR rate is the same as in iron. A similar situation has been observed in the Fe–1Cr alloy [1], where the alloy RR rate, compared to that in iron, was smaller near the I_{D1} substage and faster near the I_{D2} substage. As in the present experiment, an additional resistivity was retained above stage I in concentrated Fe–1Cr and Fe–3Cr alloys. In dilute Fe–Cr alloys, the increase in the RR observed near the I_{D2} substage is offset by the reduction in RR in the I_E substage, so that the total RR above stage I is the same as in pure iron [1]. Such effect has been found in alloys with chromium content up to 1000 ppm. The effect, like a similar one in dilute Fe–Mn alloys, had been interpreted [1, 2] to be from the formation of mixed dumbbells having a mobility slightly higher than that of self-IAs (although Mn and Cr atoms are slightly oversized in iron), as a result of which, some fraction of the I_E substage processes were shifted to lower temperatures. Above stage I temperatures in concentrated alloys, an additional retained resistivity has been explained by the trapping of mixed dumbbells in configurations of several chromium atoms located at neighbouring lattice sites. These configurations are stochastically formed in concentrated alloys.

Concerning the present alloys, the simplest form of such trapping, i.e. the simplest configuration trap, is a mixed dumbbell trapped at a single chromium atom with the possible formation of an impurity dumbbell, in contrast to FCC alloys where the mixed dumbbell is the simplest configuration trap [4]. In concentrated alloys (with a chromium concentration of a few per cent) where the distance between IAs and chromium atoms is sufficiently small,

the formation of mixed dumbbells should start at temperatures significantly below the I_E substage over the I_C and/or I_{D1} substage temperature range. Since the mobility of mixed dumbbells is higher than that of self-IAs, they should be immediately retrapped, primarily by single chromium atoms, if such a configuration is stable at this temperature. The observed suppression of the I_{D1} and I_{D2} substages with chromium concentration provides evidence for this stability over these substage temperature intervals.

The dissociation of this type of configuration trap at higher temperatures should be accompanied by the migration of mixed dumbbells, their recombination with vacancies and possibly by their trapping in the second type of configuration, which consists of two chromium atoms.

If the Fe–Cr alloys are considered as completely disordered or close to that, the concentration of chromium atom pairs can be calculated as the square of chromium concentration in the first approximation. But according to [19] the Cowley parameter of a short-range (SR) order in an Fe–5Cr alloy for the first and second coordination spheres is close to its maximum possible value after heat treatment at about 700 K. This means that the majority of Cr–Cr pairs should dissolve during such a heat treatment and the equilibrium state of SR order in two nearest coordination spheres at lower temperatures should be nearly constant and saturated. Although the heat treatment of our samples differs from the one used [19] such a strong degree of correlation between Cr atoms found in [19] should significantly reduce the number of Cr–Cr pairs as compared with the disordered state.

We have started studying the processes of thermal (at 700 K) and radiation-enhanced (at 320–420 K) SR ordering in the same alloys as in this paper by means of the Mössbauer technique [20]. The initial state of the alloys was the same as in the present paper. Our first results for the alloys close to Fe–5Cr (4Cr and 6Cr) do not provide evidence in favour of a very strong correlation between Cr atoms found in [19]†:

(a) the distribution of the Cr atoms in the initial state was close to the binomial one, i.e. typical for disordered alloys;
(b) the effect of electron irradiation on the SR ordering in the alloys, both in the initial state and after annealing at 700 K, was significantly stronger than the effect of annealing at 700 K only, i.e. the signs of saturation in the SR order degree were not observed.

Thus we can consider our Fe–Cr alloys as disordered ones and the concentration of chromium atom pairs in the Fe–2Cr alloy can be estimated as about 300 at. ppm. Therefore, the dissociation of the first type of trap will be accompanied by a sharp drop in the trap concentration, from a percentage to the range of several hundred ppm. All processes suppressed by trapping at single chromium atoms will be reactivated and limited in their effects by the total concentration of the second type of configuration (chromium pairs) and the effective residual impurity traps. In the case of our Fe–2Cr alloy, this concentration might be about 300–600 at. ppm (300 at. ppm of chromium pairs, plus 100 at. ppm of Ni, plus 200 at. ppm of interstitial impurities, but not all impurity atoms might be effective traps for mixed dumbbells). It is likely that the dissociation of Cr retrapped mixed-dumbbells occurs in the Fe–2Cr alloy near 118 K, resulting in a large RR rate. A similar conclusion follows also from the RR data in the Fe–0.1Cr alloy [1]. If the first type of configuration trap were stable, the drop in the RR rate would be observed near 118 K instead of increasing in the alloy, compared with that in iron, since the capture of migrating mixed dumbbells by 1000 ppm of Cr atoms should lead to suppression of the RR.

If the second type of configuration trap is stable and effective at the end of stage I, and if the capture is not accompanied by a significant drop in the IA resistivity, the retained resistivity

† The corresponding paper is under preparation for publication and will be submitted to *Physics of Metals and Metallography* (Russia).

at the end of stage I in the Fe–2Cr alloy should correspond approximately to the RR level in iron at the onset of the substage I_E, since a 300–600 at. ppm trap concentration should suppress almost completely IA long-range migration. Figure 1 shows that such an assumption is valid. But in the case of our Fe–2Cr alloy, the effect cannot be attributed unambiguously to the chromium atom pairs, since the impurity atoms might affect the RR in the same manner. Therefore, we have made an attempt to determine the effect of a wide range of chromium concentrations.

The main idea is to choose an addition element that provides traps for self-IAs, which will be effective above the temperature range of the stage I, and to compare the RR level at the end of stage I in iron doped with this impurity and in the alloys being investigated. The aim of this comparison is to verify whether the effect of a given concentration of the addition element is similar to the effect of the chromium pairs in the Fe–Cr alloys.

The RR level depends not only on the trap concentration but also on the parameters of trapping such as capture radius and relative drop in resistivity of a formed complex. This means that not every impurity trap effective above stage I can be used for the comparison. The only criterion in choosing the impurity is the similarity in variation of the RR with trap (impurity atom and Cr pair) concentration in iron–impurity and Fe–Cr alloys. To avoid a fortuitous correlation, the RR in the iron alloys have to be compared with that in the Fe–Cr ones over as wide a trap concentration range as possible. We have found that Fe–Mo alloys [13] are suitable for such a comparison.

One more factor can affect the RR level in Fe–Cr alloys, namely, the short-range order contribution to resistivity [19, 7], which may be due to mixed dumbbell migration [4]. The comparison of the present data and data [6] in the alloys of close composition, but with quite different irradiation-induced resistivity increments, shows that the contribution is not essential at the end of stage I.

Nevertheless, a direct comparison of the RR levels obtained in our experiment and in experiment [13] is not feasible, because the energy of the electrons was different. Therefore, we have used an indirect method. For a given RR level at 142 K on the recovery curve of the Fe–Cr alloy, we determine on the recovery curve of pure iron, irradiated under the same conditions, the temperature labelled as T_{Fe}, for which the RR level is the same; the same procedure applied to the Fe–Mo alloys (for both Fe–Mo and Fe irradiated with 1.6 MeV electrons) allows us to determine the temperature T^*_{Fe}. These two temperatures have to be compared. It is a rougher estimate than direct comparison of the RR levels, but it is less sensitive to the little known details of the RR mentioned above.

Table 2 gives a direct comparison of the RR levels at the end of stage I in the Fe–Cr and Fe–Mo alloys with similar concentrations of Cr atom pairs and Mo atoms [1, 13], irradiated with the same 1.6 MeV electrons at similar temperatures. A good correlation is observed, but only in a narrow range of Cr pair concentrations.

Table 2. Direct comparison of the RR in Fe–Cr and Fe–Mo alloys.

Fe–Cr alloy	Cr atom pair conc. in Fe–Cr alloy (at.%)	RR in Fe–Cr alloy $\Delta\rho(145\ \mathrm{K})/\Delta\rho_0$ (%)	Mo conc. in Fe–Mo alloy (at.%)	RR in Fe–Mo alloy $\Delta\rho(145\ \mathrm{K})/\Delta\rho_0$ (%)
Fe–1Cr	0.01	14–18	0.01	16
Fe–3Cr	0.09	28	0.1	28

Table 3 lists the RR levels at 142 K in our alloys, temperatures T_{Fe} and T^*_{Fe}, concentrations of Cr atom pairs and concentrations of Mo. As it can be seen from table 3, a good agreement between the two data sets over two orders of magnitude (in Mo and in Cr pair concentrations)

is also observed. Therefore, the retained resistivity at the end of stage I in irradiated Fe–Cr alloys is controlled over a wide range of chromium concentrations by the concentration of chromium atom pairs, and IAs surviving at the end of stage I are mixed dumbbells, trapped primarily at configurations of chromium atom pairs.

Table 3. Indirect comparison of the RR in Fe–Cr and Fe–Mo alloys (see details in the text).

Alloy	RR in Fe–Cr alloy $\Delta\rho(142\ \mathrm{K})/\Delta\rho_0(90\ \mathrm{K})$ (%)	T_{Fe} (K) (Fe–Cr)	Cr atom pair conc. in Fe–Cr alloy (at.%)	Mo conc. in Fe–Mo alloy (at.%)	T^*_{Fe} (K) (Fe–Mo)
Fe1	23.3				
Fe–2Cr	36.0	120	0.029	0.04	120
Fe–4Cr	47.7	113	0.16	0.10	115
Fe–6Cr	55.2	110	0.36	0.3	112
Fe–9Cr	65.9	107	0.81	1	107
Fe–11Cr	68.2	107	1.17	—	—
Fe–16Cr	70.7	104	2.56	3	103

4. Conclusions

(1) Generation of radiation-induced defects within small cascades in the 5 MeV electron-irradiated iron was found to stimulate the formation of DIAs, which either are formed directly during cascade formation and become mobile near the substage I_{D1} temperature, or are formed from close IA pairs near the substage I_{D1} temperature at which they are already mobile and can be trapped by interstitial impurity atoms.

(2) Specific features of the RR of electron-irradiated Fe–Cr concentrated alloys over the stage I temperature interval can be easily explained by the formation, the migration and the successive trapping of mixed Fe–Cr dumbbells at single and paired chromium atoms, and the surviving stage I IAs are mixed dumbbells, primarily trapped at chromium atom pairs.

Acknowledgments

This work has been supported by the Russian Foundation for Fundamental Research (grant No 98-02-17341). The author wishes to thank V A Pavlov for irradiating the samples, S E Danilov for assisting in transferring the sample holder, O and C Dimitrovs for reading the manuscript critically and making valuable suggestions and C M Elliott for editing the text.

References

[1] Maury F, Lucasson P, Lucasson A, Faudot F and Bigot J 1987 *J. Phys. F: Met. Phys.* **17** 1143
[2] Maury F, Lucasson A, Lucasson P, Loreaux Y and Moser P 1986 *J. Phys. F: Met. Phys.* **16** 523
[3] Abe H and Kuramoto E 1999 *J. Nucl. Mater.* **271–272** 209
[4] Maury F, Lucasson P, Lucasson A, Vajda P, Balanzat E, Beretz D, Halbwachs M and Hillairet J 1984 *Radiat. Eff.* **82** 141
[5] Bocquet J L 1986 *Acta Metall.* **34** 571
[6] Benkaddour A, Dimitrov C and Dimitrov O 1987 *Mater. Sci. Forum* **15–18** 1263
[7] Nikolaev A L, Arbuzov V L and Davletshin A E 1997 *J. Phys.: Condens. Matter* **9** 4385
[8] Fujii T and Morimoto I 1969 *Japan. J. Appl. Phys.* **8** 1154
[9] Kubaschewski O 1982 *Iron—Binary Phase Diagrams* (Berlin: Springer)
[10] Takaki S, Fuss J, Kugler H, Dedek U and Schultz H 1983 *Radiat. Eff.* **79** 87

[11] Dimitrov C, Benkaddour A, Corbel C and P Moser, 1991 *Ann. Chim.* **16** 319
[12] Campbell I A and Fert A 1982 *Ferromagnetic Materials* ed E P Wolhlfarth (Amsterdam: North-Holland) p 760
[13] Maury F, Lucasson A, Lucasson P, Moser P and Faudot F 1990 *J. Phys.: Condens. Matter* **2** 9269
[14] Maury F, Lucasson A, Lucasson P, Moser P and Faudot F 1990 *J. Phys.: Condens. Matter* **2** 9291
[15] Kirsanov V V 1990 *Vychislitelnyi Eksperiment v Atomnom Materialovedenii [Computer Experiment in Nuclear Material Science]* (Moscow: Energoatomisdat) pp 80–81 (in Russian)
[16] Johnson R A 1964 *Phys. Rev.* **134** A1329
[17] Lucasson P, Maury F and Lucasson A 1985 *Radiat. Eff. Lett.* **85** 219
[18] Jacques H and Robrock K H 1982 *Point Defects and Defect Interactions in Metals* ed J I Takamura, M Doyama, M Kiritani (Tokyo: University of Tokyo Press) p 159
[19] Mirebeau I, Hennion M and Parette G 1984 *Phys. Rev. Lett.* **53** 687
[20] Nikolaev A L, Filippova N P and Shabashov V A 1999 *Abstracts 3rd Int. Ural Seminar on Radiation Damage Physics of Metals and Alloys (Snezhinsk, 1999)* p 32